ACS APPLIED MATERIALS & INTERFACES

Research Article

www.acsami.org

Stretchable Carbon Nanotube/Ion–Gel Supercapacitors with High Durability Realized through Interfacial Microroughness

Jiho Lee, Wonbin Kim, and Woong Kim*

Department of Materials Science and Engineering, Korea University, Seoul 136-713, Republic of Korea

Supporting Information

ABSTRACT: A critical problem with stretchable supercapacitors developed to date has been evaporation of a volatile component of their electrolyte, causing failure. In this work, we demonstrated successful use of an ionic-liquid-based nonvolatile gel (ion–gel) electrolyte in carbon nanotube (CNT)-based stretchable supercapacitors. The CNT/ion–gel supercapacitors showed high capacitance retention (96.6%) over 3000 stretch cycles at 20% strain. The high durability against stretch cycles was achieved by introducing microroughness at the interfaces between different materials. The microroughness was produced by the simple process of imprinting the surface microstructure of office paper onto a poly(dimethylsiloxane) substrate; the surface texture is reproduced in successive current collector and CNT layers. Adhesion between the different layers was strengthened by this roughness and prevented delamination over repeated stretch cycles. The addition of a CNT layer decreased the sensitivity of electrical characteristics to stretching. Moreover, the ion–gel increases the operating voltage window (3 V) and hence the energy density. We believe our demonstration will greatly contribute to the development of flexible and/or stretchable energy-storage devices with high durability.

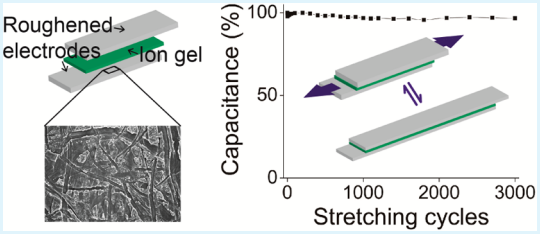

KEYWORDS: *supercapacitor, carbon nanotube, ionic liquid, microstructure, interface, adhesion, stretchability*

1. INTRODUCTION

Stretchable electronics is considered a promising class of future components that could extend a technology based on rigid materials into one including soft and/or elastic materials. While electronic devices such as sensors, light-emitting diodes, and field-effect transistors have been extensively studied in stretchable forms,[1−6] energy-conversion and -storage devices to power the electronic devices are significantly underdeveloped.[7,8] For the realization of stand-alone stretchable devices, it is essential to also develop stretchable power supplies.

A stretchable supercapacitor is an excellent candidate for a power supply in stretchable electronic devices. Especially for this application, supercapacitors have distinctive advantages over batteries. They have a simple device structure that can be readily implemented in integrated systems, excellent charge–discharge cyclability assuring low or no maintenance or replacement, and high rate capability arising from their simple working principle.[9−11] Also, they do not contain toxic or inflammable materials and have little environmental impact. Although other types of power supplies such as nanogenerators and solar cells have been recently reported,[12−15] energy-conversion devices such as these can supply power only when an external source such as solar or mechanical energy is available. Therefore, energy-storage devices such as supercapacitors can be essential as a continuous source of power for electronics, regardless of the availability of external power sources.

It is critical to develop electrolyte materials having appropriate properties such as nonvolatility and elasticity for successful stretchable supercapacitors. Nonetheless, most reports on stretchable supercapacitors have focused on the development of stretchable electrode materials and designs, with little attention having been paid to the development of electrolytes. Widely used electrolytes are generally liquid[16−18] or poly(vinyl alcohol) (PVA)-based gels.[19−24] However, liquid electrolytes are not appropriate for stretchable supercapacitors because of the intrinsic leakage problem.[25,26] Further, PVA gel electrolytes may not be suitable because water in the gel can evaporate, causing failure of the charge-storage operation.[27] Encapsulation may retard water evaporation but is not an ultimate solution. It also requires the daunting task of developing encapsulation materials that have both high stretchability and low water permeability over repeated stretch cycles.

From this perspective, ionic-liquid-based polymer gels are a promising type of electrolyte. There is no solvent-evaporation problem because ionic liquids are nonvolatile molten salts without additional solvent.[27−29] There is no leakage problem because the electrolytes are in gel form. Moreover, the conductivity of ion–gel electrolytes can be comparable to their counterpart liquid electrolytes.[25,30] Finally, ionic liquid electrolytes provide a wider operating voltage window (>3 V)

Received: May 13, 2014
Accepted: July 28, 2014
Published: July 28, 2014

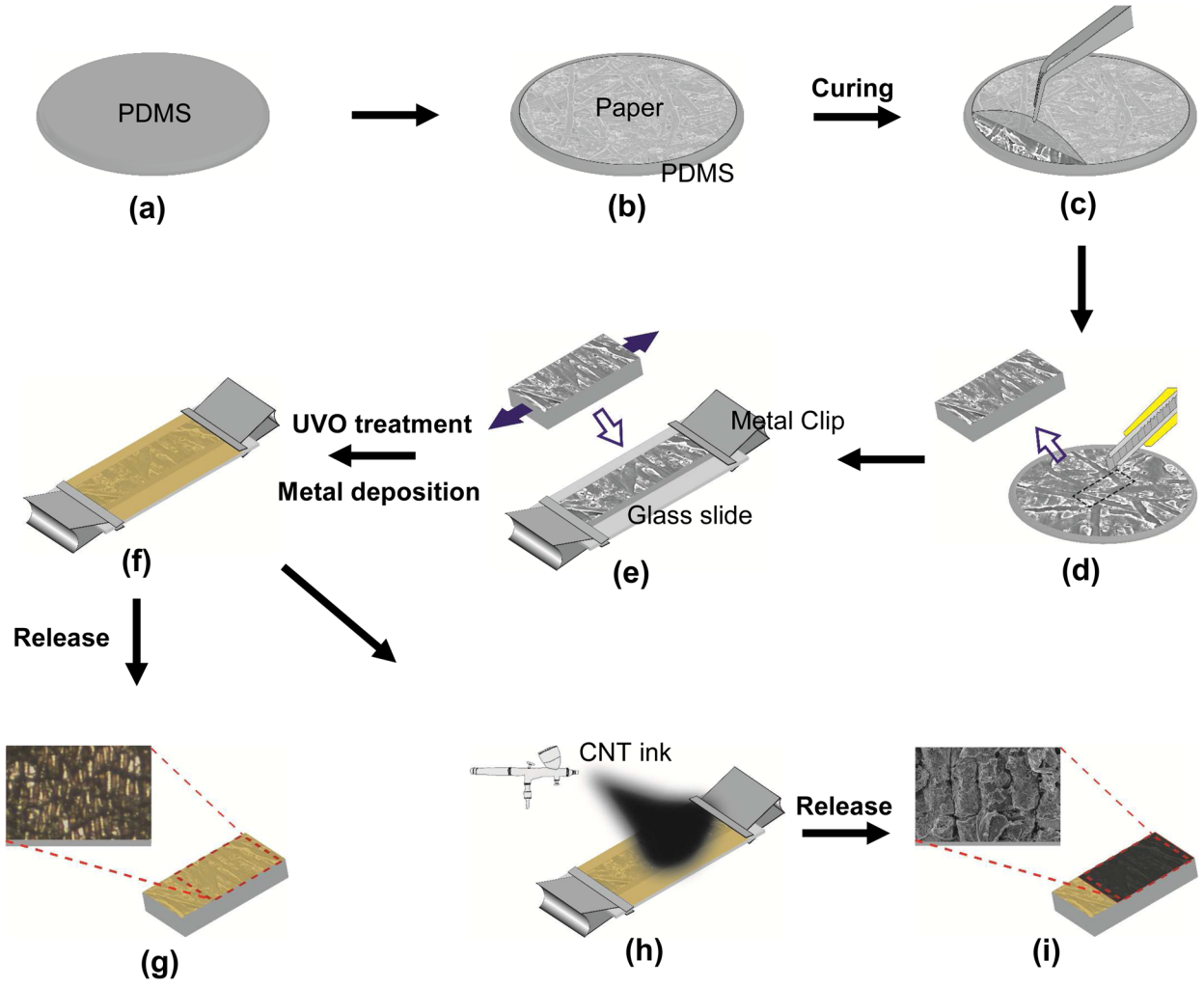

Figure 1. Schematic of the fabrication of stretchable electrodes. Steps in the process are denoted as a–i. (a) PDMS solution. (b) Transfer of the microroughness of paper onto PDMS. (c) Paper detachment after PDMS is cured. (d) Cutting the PDMS blank into the desired shape. (e) Elongation of the PDMS substrate to fabricate a buckling structure. (f) UVO surface treatment and metal deposition on a stretched substrate. (g) Metal/PDMS substrate released after deposition, showing the buckling structure. (h) CNT spray coating. (i) CNT/metal/PDMS substrate released after CNT deposition, showing the buckling structure.

than aqueous or organic electrolytes, increasing the energy density. However, 3 V stretchable supercapacitors with intrinsic high durability have not been demonstrated previously. In comparison, a stretchable supercapacitor demonstrated by Kim et al. was based on a serpentine design of interconnects and not on stretchable electrolytes.[31] Moreover, it showed very limited cyclability (~10 cycles), perhaps due to stress focused on the junctions between interconnecting electrodes and supercapacitors. Wallace et al. demonstrated an ionic-liquid-based gel electrolyte for supercapacitors but with a low operating voltage window (1 V).[32]

In this work, we demonstrate ionic-liquid/polymer-gel-based 3 V stretchable supercapacitors with high capacitance retention ($C_{areal} \sim 3$ mF/cm^2 and $C_{sp} \sim 50$ F/g) over 3000 stretch cycles (strain $\varepsilon \sim 20\%$). The stretchable ion–gel was composed of ionic liquid, 1-ethyl-3-methylimidazolium bis-(trifluoromethylsulfonyl)imide (EMIM-TFSI), and a polymer, poly(vinylidene fluoride-*co*-hexafluoropropylene) (PVDF-HFP). Carbon nanotubes (CNTs) were spray-deposited on metal-coated poly(dimethylsiloxane) (PDMS) substrates and used as electrode materials. Simple application of ion–gel onto the CNT/metal/PDMS substrate led to a delamination failure at the CNT/metal interface. To prevent delamination and promote adhesion between layers, the interfaces were microroughened. Because various materials adhere well to a paper surface owing to surface roughness and/or chemical interaction such as hydrogen bonding,[25,33] we introduced microroughness by simply transferring microstructures from the surface of regular office paper onto the PDMS substrates. The microroughness imprinted on PDMS was then conveyed to successive layers of metal and CNT deposited onto the roughened PDMS. Owing to improved interfacial strength between the layers, characteristics of the supercapacitors remained virtually constant over 3000 cycles of stretch, as evidenced from cyclic voltammograms, galvanostatic charge–discharge curves, and Nyquist plots. Moreover, the successful incorporation of ion–gel naturally led to the wide operating voltage window of 3 V owing to the high electrochemical stability of ionic liquid.

2. EXPERIMENTAL SECTION

Transferring Microstructure from Paper to a PDMS Substrate. A PDMS substrate was prepared by mixing the "base" and the "curing agent" of a silicone elastomer kit (Dow Corning,

Sylgard 184) at a volumetric ratio of 10:1. The mixture was degassed in a desiccator using a vacuum pump to remove air bubbles. The mixed solution was uniformly spread on a plastic Petri dish, and a piece of paper (Double A) was gently attached on the top surface of the spread solution, ensuring uniform contact between the paper and the viscous solution. The solution was cured at 60 °C on a hot plate for at least 12 h. The paper was easily removed from the cured PDMS, leaving the microstructure transferred from the paper surface.

Preparation of Stretchable Electrodes. The as-prepared PDMS substrate, having a microstructured or roughened surface by the paper-pattern transfer, was cut into desired shapes (50 mm × 10 mm). Each end (~7.5 mm) of the electrode strip was fixed with metal clips onto a glass slide. The 35-mm-long segment was stretched to 55 mm, an extension of around 60%. Then, the substrates were exposed to ultraviolet (UV) light (low-pressure mercury lamp, 25 mW/cm^2 at 20 mm distance, reported by the manufacturer) for 20 min in a commercial UV−ozone (UVO) chamber (Jaesung Engineering Co., UVC-30).[34] A titanium (Ti) adhesion layer (~5 nm) and a gold (Au) layer (~50 nm) were successively deposited by electron-beam evaporation. With a commercial airbrush (Style X, X-3), single-walled carbon nanotube (SWCNT) ink was sprayed on the substrates. Here, we used ink comprised of SWCNT (Sigma-Aldrich) and sodium dodecylbenzenesulfonate (SDBS) surfactant in water (both 1 mg/mL). Prior to use, the ink was bath-sonicated for 5 min and bar-sonicated (Sonics & Materials, VC 750) for 20 min. The substrates were placed on a heated hot plate to evaporate water from the sprayed ink. By removal of the metal clips after CNT deposition, the prestrain was released. Shrinkage of the PDMS substrate led to formation of the buckling structure of the SWCNT network/Au layer.

Preparation of Stretchable Polymer Gel Electrolytes. The solution-casting method was used to form the electrolyte layers.[29] PVDF-HFP (Sigma-Aldrich, 0.3265 g) was dissolved in acetone (5.5 mL) and EMIM-TFSI (C-TRI Co., 0.5 mL). The mixture was magnetically stirred for at least 60 min at 400 rpm, until the polymer particles were completely dissolved and the solution became homogeneous. Evaporation of the acetone results in the formation of solvent-free stretchable electrolytes (Supporting Information, Figure S1). Polymer gel electrolytes were cast in a standard "dumbbell"-shaped mold (ASTM D412-A type) for testing of the mechanical properties.

Assembly of Stretchable Supercapacitors. A stretchable supercapacitor was assembled with two CNT/metal/PDMS electrodes and an ion−gel electrolyte layer between the electrodes (Supporting Information, Figure S2). First, the electrolyte solution was cast on the active surface of a pair of preelongated CNT electrodes. Evaporation of the acetone solvent in a dry atmosphere led to the formation of a solvent-free gel electrolyte layer on each electrode. Multiple casting was performed to achieve the desired thickness (~0.5 mm) and to prevent an electrical short between electrodes. Then, on one of the electrolyte-coated electrodes, another layer of electrolyte was cast to act as an adhesive. While the solution was still viscous, the other electrolyte-coated electrode was firmly pressed on it until acetone in the adhesive layer had evaporated and the whole supercapacitor became solidified.

Characterization. Surface images of the buckled Au film on PDMS were captured at different tensile strains, using a camera installed in an optical microscope (INUTRA, zoom video microscope system) and a custom-made stretcher for the electrode samples. The morphology of CNT-coated electrodes was observed using a field-emission scanning electron microscope (Carl Zeiss, AURIGA). For the CNT adhesion test, a probe tack method was employed using a cylindrical probe with planar contact (diameter = 5 mm). Both descending and ascending speeds were set to 1 mm/s, and the compression force was set to 300 g force (gf) with 10 s duration (Yeonjin Corp., TXA). The mechanical properties of the gel electrolytes were measured using a universal testing machine (Tinius Olsen, H5K-T), with the test speed set to 50 mm/min. The electrochemical properties were measured in an argon-circulating glovebox (Korea Kiyon, KK-021-AS) using an electrochemical analyzer (BioLogic, VSP-300). Curve fitting was performed with EC-Lab software (BioLogic).

3. RESULTS AND DISCUSSION

The fabrication process of stretchable electrodes with microroughness is illustrated in Figure 1. First, the surface microstructure of office paper is transferred onto a PDMS substrate by simple curing of a PDMS precursor solution with the paper placed on it (a and b). After PDMS was cured, the paper was detached, leaving a microstructure on PDMS (c). Then, PDMS was cut into a desired shape (50 mm × 10 mm; d). Next, buckling structures were imposed on microroughened PDMS to add stretchability to the electrodes. A buckling structure was created by depositing electrode materials such as Ti, Au, and CNTs on a stretched PDMS blank and releasing the tensile stress after deposition.[16,35] The substrate was stretched to a strain of around 60%, and Ti and Au successively evaporated onto it (e and f). An Au/Ti-deposited stretchable electrode was released from strain and set aside as a comparison sample (g). Finally, a CNT layer was spray-coated on Au/Ti/PDMS (h). After release, buckling structures were formed in both cases (g and i).

The surface microstructure from the office paper sample was successfully imprinted onto the PDMS layer. Because paper is a mat of cellulose fibers (diameter ~10 μm), the paper surface has a corresponding micrometer-scale roughness.[33] A scanning electron microscopy (SEM) image of the paper surface shows the protrusion of cellulose fibers (Figure 2a). Accordingly,

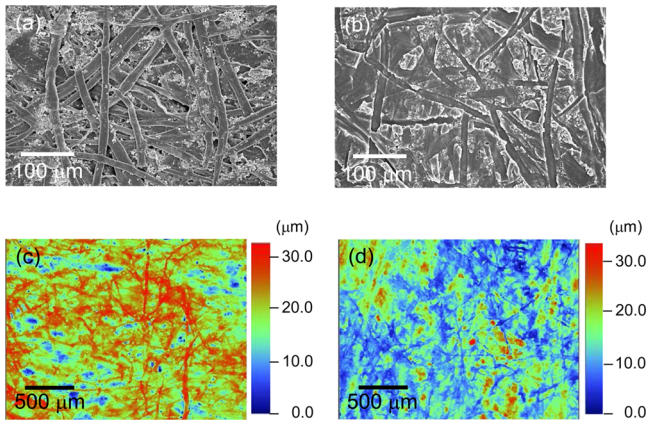

Figure 2. SEM images of (a) microstructures on commercial office paper and (b) microstructures imprinted on cured PDMS. Surface profile images of (c) commercial office paper and (d) the imprinted PDMS.

indented structures appear on the cured PDMS substrate (Figure 2b). For visualization, surface profiles of the paper and PDMS were optically scanned and expressed with color gradient, as shown in parts c and of Figure 2, respectively. Both profiles vertically span around 32−33 μm from the lowest to the highest points. Protruding structures on the paper surface are shown in red on the optical profile image; indented structures on the PDMS sample are visualized in blue. The characteristic dimensions of microstructures on PDMS such as the width and depth match well with those of the original structures on paper. The results clearly indicate that the PDMS surface structures are inherited from the paper template.

We investigated surface morphologies of the electrodes with and without microroughness, stretched to various degrees for

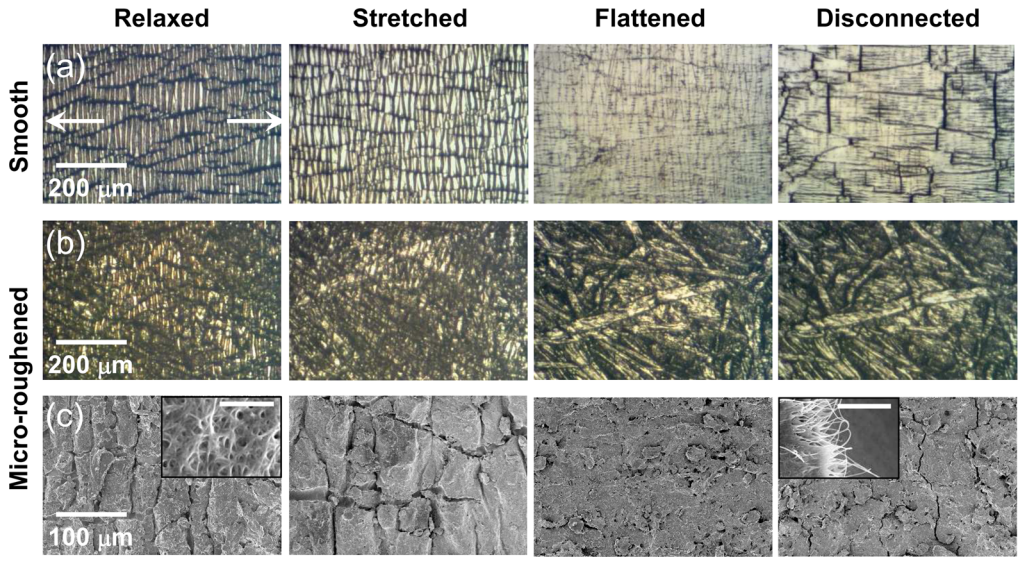

Figure 3. Surface morphologies of (a) a metal/PDMS electrode without imprinted microroughness and (b) metal/PDMS and (c) CNT/metal/PDMS both with microroughness. Surface types (a–c) are shown at various strain levels. Buckling structures are shown on both electrodes at a relaxed state. They fade away as the electrode is stretched and disappear at a prestrain level (flattened). Microroughness is clearly shown on the paper-patterned PDMS. When the electrode is stretched beyond the prestrain level, cracks perpendicular to the stretch direction appear (disconnected). Arrows indicate the stretch direction. Insets in part c: CNT network on the relaxed CNT/metal/PDMS (scale bar = 400 nm) and CNTs at the edge of a crack generated from excessive tensile deformation (scale bar = 1 μm).

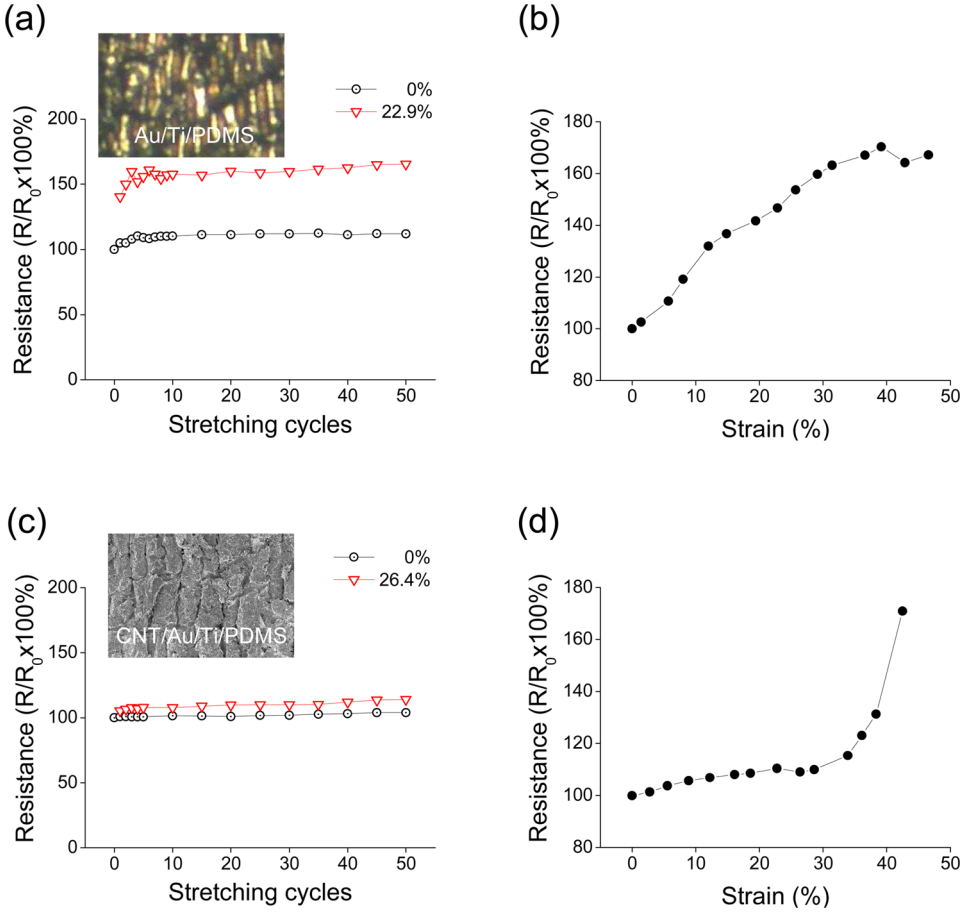

Figure 4. Normalized electrical resistances of a metal/PDMS electrode: (a) measured at released and stretched states over 50 stretch cycles and (b) measured at different tensile strains. Inset: photograph of metal/PDMS. Normalized electrical resistances of a CNT/metal/PDMS electrode: (c) measured at released and stretched states over 50 stretch cycles and (d) measured at different tensile strains. Inset: SEM image of CNT/metal/PDMS. The resistance (R) measured at stretched/released states of each cycle was normalized by the resistance (R_0) measured before the first stretch (i.e., cycle 0).

dx.doi.org/10.1021/am502953g | ACS Appl. Mater. Interfaces 2014, 6, 13578–13586

examination. Because Au was evaporated onto PDMS at a prestrain of approximately 60%, the buckling structure was formed when the electrodes returned to a relaxed state. Without microroughness, the buckling structure of an Au/Ti/PDMS electrode is clearly shown as lines perpendicular to the stretch/release direction with a pitch of a couple of tens of micrometers (Figure 3a). Together with the buckling structures, cracks were observed along the stretch direction. When PDMS is stretched for metal deposition, a reduction in its width follows; upon release, the width of PDMS expands to its original size, applying a tensile stress to the added material. This process generates cracks in the Au/Ti film along the stretch direction (indicated as relaxed). As the Au/Ti/PDMS electrode is stretched, the pitch of the buckling structure increases (stretched). When the strain approaches the level of prestrain, features including the buckling structure and cracks fade away and the surface becomes flat (flattened). Finally, when the Au layer is stretched beyond the prestrain level, cracks perpendicular to the stretch direction appear, leading to electrical and mechanical disconnection (disconnected).

On the other hand, Au/Ti/PDMS with microroughness also shows similar features at the four distinct stages of strain, with the paper patterns overlaid on them (Figure 3b,c). In particular, when the electrode reaches the flattened state, the clean-cut pattern transferred from paper can be seen because all other features have nearly disappeared. Finally, the CNT electrode (CNT/Au/Ti/PDMS) with microroughness also shows a similar trend in the change of morphologies (Figure 3c).

The CNTs bridge the mechanical gaps of the metal layer and reduce resistance variations during the stretching process. Upon being stretched (ε = 22.9%), the Au/Ti/PDMS electrode shows resistance levels of approximately 14 and 21 Ω for relaxed and stretched states, respectively, through 50 stretch cycles (Figure 4a). Resistance increased proportionally to strain, for the range of ε = 0−50%, up to approximately 170% of the unstrained value, as shown in Figure 4b. On the other hand, the presence of CNTs on the metal electrode significantly reduced the resistance variation (Figure 4c). The change in the resistance was within ∼10% over 50 cycles of stretch for a strain of 26.4%. That resistance change was generally maintained for strains of up to 30% and then sharply increased, as shown in Figure 4d. The results show that the CNTs play a critical role in maintaining the conductance of the electrode against repeated stretches. This can be attributed to the CNT network forming bridges over local gaps of the metal electrodes opened upon being stretched and thus maintaining electrical paths.

An adhesion test confirmed that microroughness indeed enhanced the interfacial strength between the layers. We performed a probe tack test to compare the adhesion of conductive layers (CNT/Au/Ti) on a smooth PDMS surface and that on a roughened PDMS surface (Figure 5). A cylindrical probe (diameter ∼5 mm) was programmed to descend, stop, stay, and ascend during a certain period of time. Double-sided adhesive tape was applied to the bottom end of the probe. The sample was firmly fixed on a planar stage. A profile of the load on the probe during the test period and the status of the probe at each step are presented in Figure 5. As the probe descends, the load remains at 0 gf until it touches the sample (a). The probe descends further until the magnitude of the load increases to approximately 300 gf (=2.94 N; b). Then, the probe stops and is held for 10 s (c). This step is to ensure firm contact between the probe and the sample. The probe ascends and the load increases in the opposite direction until

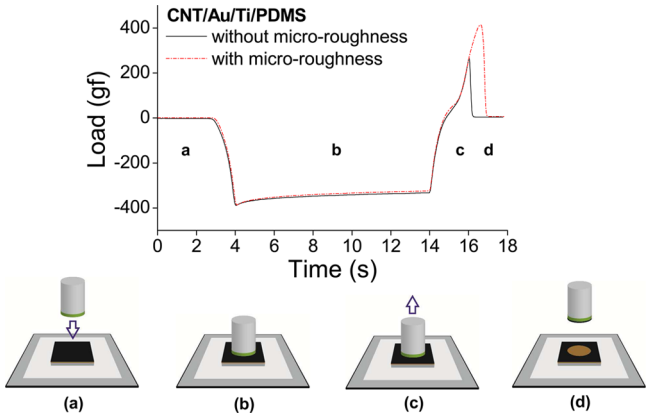

Figure 5. Probe tack test on CNT/Au/Ti/PDMS with and without imprinted microroughness. Load profiles are shown at different stages: (a) lowering the probe until the load reaches a specified value; (b) holding the probe at the specified load value for a certain period of time; (c) raising the probe; (d) detachment occurring at different load levels, depending on the adhesion strengths. Each step is illustrated and denoted in the load profile.

the CNT layer detaches from the metal layer (d). Once detachment occurs, the load becomes 0 gf. Detachment occurred at the interface between the CNT and metal layers in both smooth and rough samples; the forces required to detach the CNT layer were 266 and 415 gf, respectively. The result confirms that microroughness enhances the interfacial strength between CNT and the metal layer by 1.5 times. Moreover, it was not even possible to fabricate the ion−gel-based supercapacitor cells without introducing the paper-induced roughness. The CNT layer spontaneously detached during solvent evaporation of the electrolyte precursor solution applied to the CNT/Au/Ti/PDMS substrate. More specifically, the CNT/buckled metal interface could not withstand the compressive stress exerted by shrinkage of the polymer gel electrolyte due to acetone solvent evaporation during the gel formation process. The introduction of microroughness enabled us to successfully fabricate supercapacitors with the ionic-liquid-based gel electrolyte.

The gel electrolyte showed elastic behaviors within the 20% strain range. The electrolyte was prepared by simple blending of EMIM-TFSI ionic liquid with PVDF-HFP polymer. The ionic liquid acted as a plasticizer, and hence the resulting mixture was highly deformable compared to a pure PVDF-HFP sample. as shown in Figure 6a.[29] The gel electrolyte was essentially elastic under repetitive strains at 20%, except for the first cycle of the stretch. More specifically, the gel was permanently elongated by 2% after the first stretch but showed almost identical stress-to-strain response for the following stretching cycles (Figure 6b,c). Figure 6c shows the stress value measured at the strain of 10% over 25 stretch cycles, showing that there is no significant change in the stress-to-strain response after the second cycle. An elastic modulus of ∼4.5 MPa indicates that this gel electrolyte is a suitable candidate for stretchable supercapacitor applications. We emphasize that the gel electrolyte is leakage-free, as manifested by its free-standing characteristic shown in Supporting Information, Figure S1.

The supercapacitor fabricated during this investigation (see below) accommodated a tensile strain of 20% with little variation in the electrochemical properties. The supercapacitor performance is almost unaffected, as indicated by the overlap of the cyclic voltammetry (CV) curves before and during the

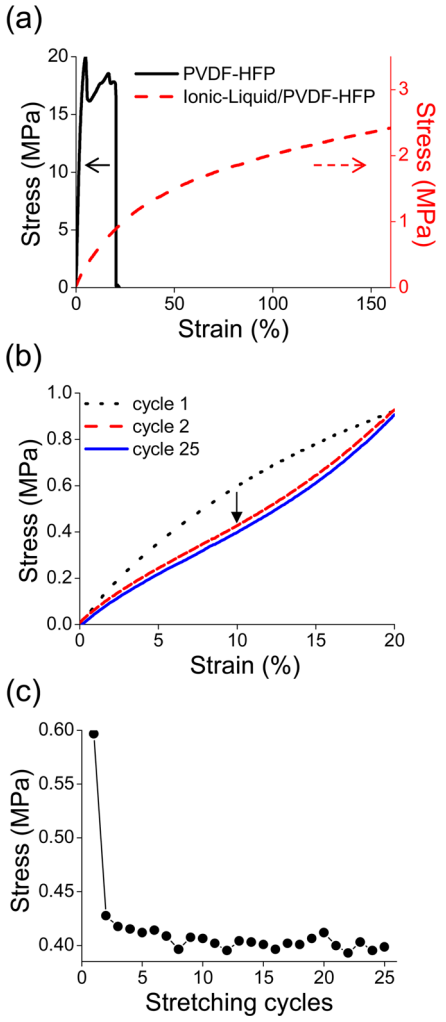

Figure 6. Stretchable gel electrolyte stress–strain curves: (a) stress–strain curves of pure PVDF-HFP polymer and an ionic liquid/PVDF-HFP gel electrolyte; (b) stress–strain curve of an ionic liquid/PVDF-HFP gel electrolyte measured at the 1st, 2nd, and 25th stretch cycle at a strain of 20%; (c) plots of stress values, read at 10% strain for the specified cycle (the arrow in part b indicates the reading point).

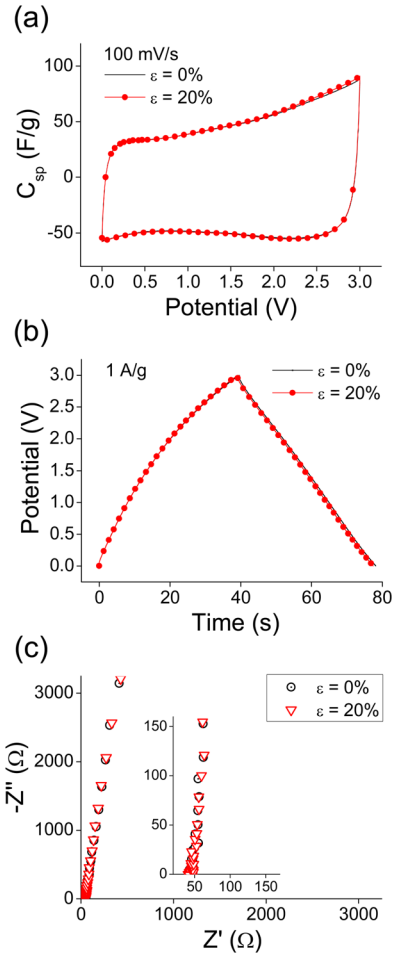

Figure 7. Supercapacitor characteristics for 20% strain: (a) cyclic voltammogram curves measured at a scan rate of 100 mV/s; (b) galvanostatic charge–discharge curve measured at a current density of 1 A/g; (c) Nyquist plots of the stretchable supercapacitor at a relaxed (ε = 0%) and a stretched (ε = 20%) state. The inset in part c shows ESRs measured. Z' and Z'' are real and imaginary impedances, respectively (frequency range: 10 mHz to 200 kHz).

stretch (ε = 20%; Figure 7a). The retention of characteristics is also observed in galvanostatic charge–discharge curves (Figure 7b). Upon stretching, the areal cell capacitance (C_{areal}) and specific electrode capacitance (C_{sp}) increased only slightly, from 2.88 mF/cm^2 and 51.8 F/g to 2.91 mF/cm^2 and 52.2 F/g, respectively (Figure 7b). The capacitances were calculated from the galvanostatic charge–discharge curve measured at 1 A/g, based on the equations $C_{cell} = I/(\Delta V/\Delta t)$, $C_{areal} = C_{cell}/A$, and $C_{sp} = 2C_{cell}/m$, where I, $\Delta V/\Delta t$, A, and m are the applied current, slope of the discharge curve after IR drop, active area ($A \sim 2.8$ cm^2), and CNT mass on an electrode ($m \sim 0.31$ mg), respectively.[25]

We notify that the energy density of our supercapacitors (~15.7 W·h/kg) is higher by several factors or even 1 order of magnitude than those of other CNT-based stretchable electrical double-layer capacitors (EDLCs; Table 1).[16,17,20] We attribute the enhanced energy density mainly to the increased operating window by ion–gel electrolytes (=3 V).[28] Moreover, our EDLC has as even comparable energy density to and higher rate capability than those of stretchable pseudosupercapacitors.[23,24]

Equations used to calculate the capacitance, energy density, and power density were presented as Supporting Information.

From the Nyquist plot, it was observed that both the equivalent series resistance (ESR) and overall frequency response of the cell in a relaxed and a stretched state were almost the same (Figure 7c). The ESR was estimated to be about 45 Ω in both relaxed and stretched states. The excellent stretchability is owing to the enhanced interfacial strength to accommodate the various materials with different properties used in the supercapacitors.

The supercapacitor showed excellent durability against repetitive stretches. Even after 3000 cycles of stretch (at ε = 20%), the electrochemical properties of the supercapacitors were well conserved. For example, the shape of the CV curves was generally maintained except that the slope of the curves at 0 and 3 V, where the sweep direction changes and becomes slightly less steep (Figure 8a). This reduction in slope could be attributed to the increase in ESR after 3000 cycles of stretch. Consistently, the increases in both the IR drop and ESR can be seen in the galvanostatic charge–discharge curves and Nyquist plots, while the general shapes of the curves are maintained, indicating negligible change in the capacitance (Figure 8b,c).

dx.doi.org/10.1021/am502953g | ACS Appl. Mater. Interfaces 2014, 6, 13578–13586

Table 1. Performance Comparison of Stretchable Supercapacitors

type	electrode	electrolyte	V^a (V)	C_{sp} (F/g)	C_{areal} (mF/cm^2)	$E_{cell}{}^b$ (W·h/kg)	$P_{cell}{}^b$ (kW/kg)	2 m_{area} (mg/cm^2)	ref
EDLC	SWNT	ion gel	3.0	51.8 (at 1 A/g)	2.88	15.7	1.48	0.222	this work
				42.8 (at 10 A/g)	2.39	9.59	12.7		
	SWNT	liquid ($TEABF_4$/PC)	1.5	54 (at 1 A/g)	0.122^c	3.81	0.33	0.009^d	16
	SWNT	liquid ($TEABF_4$/PC)	1.5	44 (at 10 A/g)	2.64	3.24	1.56	0.24	17
	SWNT	H_2SO_4/PVA gel	0.8	48 (at 10 A/g)	0.43^c	0.98	0.96	0.036^d	20
pseudocapacitor	polyaniline/graphene	H_3PO_4/PVA gel	0.8	405 (at 0.75 A/g)	135^c	9.0^e	0.33	1.33	23
	polyaniline/MWCNT	H_2SO_4/PVA gel	0.8	495 (at 1.89 A/g)	131^c	11^e	0.8	1.06	24

$^a V$ is the operating voltage window. $^b \Delta V$ and Δt are read from the galvanostatic charge−discharge curves provided in references. $^c C_{areal}$ is the capacitance per unit area of a cell ($=C_{sp}/4 \times 2m_{areal}$). $^d m_{areal}$ is the areal mass of electrode materials and estimated by mutiplying the thickness and the gravimetric density of the electrode materials. $^e V$ was used instead of ΔV.

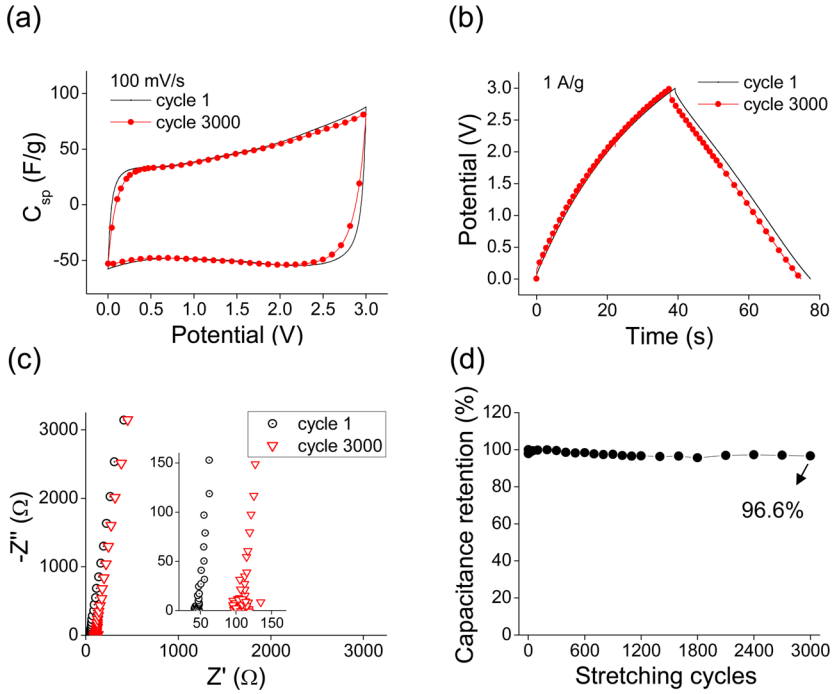

Figure 8. Supercapacitor characteristics at 3000 stretch cycles: (a) CV curves; (b) galvanostatic charge−discharge curves; (c) Nyquist plots measured at the 1st and 3000th stretch cycles. See Figure 7 for notes. (d) Capacitance retention over 3000 stretch cycles.

Furthermore, the galvanostatic charge−discharge curves measured at various current densities confirm the high rate capability of the supercapacitors (Supporting Information, Figure S3).

Above all, 96.6% of the initial capacitance was retained over 3000 stretch cycles, as shown in Figure 8d. Additionally, we established an equivalent circuit, of which the impedance is composed of a series resistance and an impedance of constant phase element (Supporting Information, Figure S4). The curve-fitting results indicate that this model agrees well with the experimental data over the whole frequency range. Our results clearly indicate that high durability of stretchable supercapacitors can be achieved by the microroughness at the interfaces.

4. CONCLUSION

We fabricated and tested a 3 V stretchable supercapacitor with a nonvolatile gel electrolyte. The supercapacitor showed high capacitance retention (96.6%) over 3000 stretch cycles at 20% strain. The supercapacitor consisted of a CNT electrode, an Au/Ti current collector, an EMIM-TFSI/PVDF-HFP gel electrolyte, and a PDMS substrate. To enhance adhesion between layers of different materials, the microroughness of regular office paper was transcribed to the PDMS substrates by imprint and conveyed to current collector and electrode materials successively deposited onto PDMS. The introduction of surface microroughness was crucial to enhancing interfacial strength and thus to realizing highly durable ion−gel-based supercapacitors without delamination problems. While transfer of the paper surface microstructure is facile, inexpensive, and scalable, more elaborate techniques such as lithography may be applied to understand better enhancement of the adhesion

property by interfacial structure and to find more optimized conditions in the future. Our novel design concept and approach may contribute to the development of various devices utilizing deformable/compliant materials and components.

■ ASSOCIATED CONTENT

Supporting Information

Photograph of free-standing elastic gel electrolytes, illustration of the assembly process of stretchable supercapacitors, equations applied to estimate the cell performances, the charge−discharge data at different current densities, and an equivalent circuit model and the corresponding curve-fitting data. This material is available free of charge via the Internet at http://pubs.acs.org.

■ AUTHOR INFORMATION

Corresponding Author

*E-mail: woongkim@korea.ac.kr.

Author Contributions

The manuscript was written through contributions of all authors. All authors have given approval to the final version of the manuscript.

Notes

The authors declare no competing financial interest.

■ ACKNOWLEDGMENTS

This work was supported by the National Research Foundation of Korea (Grant NRF-2011-0023727).

■ REFERENCES

(1) Kaltenbrunner, M.; Sekitani, T.; Reeder, J.; Yokota, T.; Kuribara, K.; Tokuhara, T.; Drack, M.; Schwödiauer, R.; Graz, I.; Bauer-Gogonea, S. An Ultra-Lightweight Design for Imperceptible Plastic Electronics. *Nature* **2013**, *499*, 458−463.

(2) Lipomi, D. J.; Vosgueritchian, M.; Tee, B. C.; Hellstrom, S. L.; Lee, J. A.; Fox, C. H.; Bao, Z. Skin-like Pressure and Strain Sensors Based on Transparent Elastic Films of Carbon Nanotubes. *Nat. Nanotechnol.* **2011**, *6*, 788−792.

(3) Sekitani, T.; Nakajima, H.; Maeda, H.; Fukushima, T.; Aida, T.; Hata, K.; Someya, T. Stretchable Active-Matrix Organic Light-Emitting Diode Display Using Printable Elastic Conductors. *Nat. Mater.* **2009**, *8*, 494−499.

(4) White, M. S.; Kaltenbrunner, M.; Głowacki, E. D.; Gutnichenko, K.; Kettlgruber, G.; Graz, I.; Aazou, S.; Ulbricht, C.; Egbe, D. A.; Miron, M. C. Ultrathin, Highly Flexible and Stretchable PLEDs. *Nat. Photonics* **2013**, *7*, 811−816.

(5) Xu, F.; Wu, M.-Y.; Safron, N. S.; Roy, S. S.; Jacobberger, R. M.; Bindl, D. J.; Seo, J.-H.; Chang, T.-H.; Ma, Z.; Arnold, M. S. Highly Stretchable Carbon Nanotube Transistors with Ion Gel Gate Dielectrics. *Nano Lett.* **2014**, *14*, 682−686.

(6) Chae, S. H.; Yu, W. J.; Bae, J. J.; Dinh Loc, D.; Perello, D.; Jeong, H. Y.; Quang Huy, T.; Thuc Hue, L.; Quoc An, V.; Yun, M.; Duan, X.; Lee, Y. H. Transferred Wrinkled Al_2O_3 for Highly Stretchable and Transparent Graphene−Carbon Nanotube Transistors. *Nat. Mater.* **2013**, *12*, 403−409.

(7) Song, Z.; Ma, T.; Tang, R.; Cheng, Q.; Wang, X.; Krishnaraju, D.; Panat, R.; Chan, C. K.; Yu, H.; Jiang, H. Origami Lithium-Ion Batteries. *Nat. Commun.* **2014**, *5*, 3140.

(8) Xu, S.; Zhang, Y.; Cho, J.; Lee, J.; Huang, X.; Jia, L.; Fan, J. A.; Su, Y.; Su, J.; Zhang, H.; Cheng, H.; Lu, B.; Yu, C.; Chuang, C.; Kim, T.; Song, T.; Shigeta, K.; Kang, S.; Dagdeviren, C.; Petrov, I.; Braun, P. V.; Huang, Y.; Paik, U.; Rogers, J. A. Stretchable Batteries with Self-Similar Serpentine Interconnects and Integrated Wireless Recharging Systems. *Nat. Commun.* **2013**, *4*, 1543.

(9) Arico, A. S.; Bruce, P.; Scrosati, B.; Tarascon, J. M.; Van Schalkwijk, W. Nanostructured Materials for Advanced Energy Conversion and Storage Devices. *Nat. Mater.* **2005**, *4*, 366−377.

(10) Miller, J. R.; Simon, P. Electrochemical Capacitors for Energy Management. *Science* **2008**, *321*, 651−652.

(11) Simon, P.; Gogotsi, Y. Materials for Electrochemical Capacitors. *Nat. Mater.* **2008**, *7*, 845−854.

(12) Lee, J. H.; Lee, K. Y.; Gupta, M. K.; Kim, T. Y.; Lee, D. Y.; Oh, J.; Ryu, C.; Yoo, W. J.; Kang, C. Y.; Yoon, S. J. Nanogenerators: Highly Stretchable Piezoelectric−Pyroelectric Hybrid Nanogenerator. *Adv. Mater.* **2014**, *26*, 820−820.

(13) Lee, J.-H.; Lee, K. Y.; Kumar, B.; Nguyen Thanh, T.; Lee, N.-E.; Kim, S.-W. Highly Sensitive Stretchable Transparent Piezoelectric Nanogenerators. *Energy Environ. Sci.* **2013**, *6*, 169−175.

(14) Lipomi, D. J.; Bao, Z. Stretchable, Elastic Materials and Devices for Solar Energy Conversion. *Energy Environ. Sci.* **2011**, *4*, 3314−3328.

(15) Lipomi, D. J.; Tee, B. C. K.; Vosgueritchian, M.; Bao, Z. Stretchable Organic Solar Cells. *Adv. Mater.* **2011**, *23*, 1771−1775.

(16) Yu, C.; Masarapu, C.; Rong, J.; Wei, B.; Jiang, H. Stretchable Supercapacitors Based on Buckled Single-Walled Carbon Nanotube Macrofilms. *Adv. Mater.* **2009**, *21*, 4793−4797.

(17) Li, X.; Gu, T.; Wei, B. Dynamic and Galvanic Stability of Stretchable Supercapacitors. *Nano Lett.* **2012**, *12*, 6366−6371.

(18) Yue, B.; Wang, C.; Ding, X.; Wallace, G. G. Polypyrrole Coated Nylon Lycra Fabric as Stretchable Electrode for Supercapacitor Applications. *Electrochim. Acta* **2012**, *68*, 18−24.

(19) Chen, X.; Qiu, L.; Ren, J.; Guan, G.; Lin, H.; Zhang, Z.; Chen, P.; Wang, Y.; Peng, H. Novel Electric Double-Layer Capacitor with a Coaxial Fiber Structure. *Adv. Mater.* **2013**, *25*, 6436−6441.

(20) Niu, Z.; Dong, H.; Zhu, B.; Li, J.; Hng, H. H.; Zhou, W.; Chen, X.; Xie, S. Highly Stretchable, Integrated Supercapacitors Based on Single-Walled Carbon Nanotube Films with Continuous Reticulate Architecture. *Adv. Mater.* **2013**, *25*, 1058−1064.

(21) Yang, Z.; Deng, J.; Chen, X.; Ren, J.; Peng, H. A Highly Stretchable, Fiber-Shaped Supercapacitor. *Angew. Chem., Int. Ed.* **2013**, *52*, 13453−13457.

(22) Zhao, C.; Wang, C.; Yue, Z.; Shu, K.; Wallace, G. G. Intrinsically Stretchable Supercapacitors Composed of Polypyrrole Electrodes and Highly Stretchable Gel Electrolyte. *ACS Appl. Mater. Interfaces* **2013**, *5*, 9008−9014.

(23) Xie, Y.; Liu, Y.; Zhao, Y.; Tsang, Y. H.; Lau, S. P.; Huang, H.; Chai, Y. Stretchable All-Solid-State Supercapacitor with Wavy Shaped Polyaniline/Graphene Electrode. *J. Mater. Chem. A* **2014**, *2*, 9142−9149.

(24) Yu, M.; Zhang, Y.; Zeng, Y.; Balogun, M.-S.; Mai, K.; Zhang, Z.; Lu, X.; Tong, Y. Water Surface Assisted Synthesis of Large-Scale Carbon Nanotube Film for High-Performance and Stretchable Supercapacitors. *Adv. Mater.* **2014**, *26*, 4724−4729.

(25) Kang, Y. J.; Chung, H.; Han, C.-H.; Kim, W. All-Solid-State Flexible Supercapacitors Based on Papers Coated with Carbon Nanotubes and Ionic-Liquid-Based Gel Electrolytes. *Nanotechnology* **2012**, *23*, 065401.

(26) Lu, W.; Henry, K.; Turchi, C.; Pellegrino, J. Incorporating Ionic Liquid Electrolytes into Polymer Gels for Solid-State Ultracapacitors. *J. Electrochem. Soc.* **2008**, *155*, A361−A367.

(27) Yang, X.; Zhang, F.; Zhang, L.; Zhang, T.; Huang, Y.; Chen, Y. A High-Performance Graphene Oxide-Doped Ion Gel as Gel Polymer Electrolyte for All-Solid-State Supercapacitor Applications. *Adv. Funct. Mater.* **2013**, *23*, 3353−3360.

(28) Armand, M.; Endres, F.; MacFarlane, D. R.; Ohno, H.; Scrosati, B. Ionic-Liquid Materials for the Electrochemical Challenges of the Future. *Nat. Mater.* **2009**, *8*, 621−629.

(29) Xu, J. J.; Ye, H.; Huang, J. Novel Zinc Ion Conducting Polymer Gel Electrolytes Based on Ionic Liquids. *Electrochem. Commun.* **2005**, *7*, 1309−1317.

(30) Kang, Y. J.; Chun, S.-J.; Lee, S.-S.; Kim, B.-Y.; Kim, J. H.; Chung, H.; Lee, S.-Y.; Kim, W. All-Solid-State Flexible Supercapacitors Fabricated with Bacterial Nanocellulose Papers, Carbon Nanotubes, and Triblock-Copolymer Ion Gels. *ACS Nano* **2012**, *6*, 6400−6406.

(31) Kim, D.; Shin, G.; Kang, Y. J.; Kim, W.; Ha, J. S. Fabrication of a Stretchable Solid-State Micro-Supercapacitor Array. *ACS Nano* **2013**, *7*, 7975−7982.
(32) Saricilar, S.; Antiohos, D.; Shu, K.; Whitten, P. G.; Wagner, K.; Wang, C.; Wallace, G. G. High Strain Stretchable Solid Electrolytes. *Electrochem. Commun.* **2013**, *32*, 47−50.
(33) Hu, L.; Choi, J. W.; Yang, Y.; Jeong, S.; La Mantia, F.; Cui, L.-F.; Cui, Y. Highly Conductive Paper for Energy-Storage Devices. *Proc. Natl. Acad. Sci. U. S. A.* **2009**, *106*, 21490−21494.
(34) Efimenko, K.; Wallace, W. E.; Genzer, J. Surface Modification of Sylgard-184 Poly(dimethyl Siloxane) Networks by Ultraviolet and Ultraviolet/Ozone Treatment. *J. Colloid Interface Sci.* **2002**, *254*, 306−315.
(35) Lacour, S. P.; Wagner, S.; Huang, Z. Y.; Suo, Z. Stretchable Gold Conductors on Elastomeric Substrates. *Appl. Phys. Lett.* **2003**, *82*, 2404−2406.